

## Template Approach for Novel Magnetic–Ferroelectric Nanocomposites

Luc Piraux<sup>1\*</sup>, Gaël Hamoir<sup>1</sup>, Ming-Wei Lee<sup>1</sup>, Etienne Ferain<sup>1,2</sup>, Alain M. Jonas<sup>1</sup>,  
Isabelle Huynen<sup>3</sup>, and Joaquín De La Torre Medina<sup>4</sup>

<sup>1</sup>*Institute of Condensed Matter and Nanosciences, Université Catholique de Louvain,  
Place Croix du Sud 1, B-1348, Louvain-la-Neuve, Belgium*

<sup>2</sup>*it4ip s.a., rue J. Bordet (Z. I. C), 7180 Seneffe, Belgium*

<sup>3</sup>*Information and Communications Technologies, Electronics and Applied Mathematics, Université Catholique de Louvain,  
Place du Levant 3, B-1348, Louvain-la-Neuve, Belgium*

<sup>4</sup>*Instituto de Física, Universidad Autónoma de San Luis Potosí, Av. Manuel Nava 6, Zona Universitaria,  
78290 San Luis Potosí, SLP, Mexico*

Received August 13, 2011; accepted October 6, 2011; published online October 25, 2011

Ni nanowires were electrodeposited into track-etched ferroelectric poly(vinylidene difluoride) (PVDF) polymer nanoporous templates to make multiferroic nanostructured composites. Using ferromagnetic resonance measurements under static voltage bias, we demonstrate a magnetoelectric effect arising from a mechanical coupling between the magnetostrictive and piezoelectric phases. The calculated electric field lines and intensity indicate that PVDF matrix surrounding the surface of the Ni nanowires experiences shear stress. The competing magnetoelastic anisotropy originating from the piezoelectric effects leads to a reduced magnetic anisotropy field along the wire axis. The nanowires packing in the array are found to play a dominant role in the magnetoelectric effect. © 2011 The Japan Society of Applied Physics

Arrays of parallel magnetic nanowires (NWs) embedded in non-magnetic dielectric media are of considerable interest for fundamental physics studies and for their possible exploitations in relevant applications such as patterned media for magnetic storage,<sup>1)</sup> nonreciprocal microwave devices,<sup>2–5)</sup> and spin-transfer torque devices.<sup>6,7)</sup> Besides this, tuning the properties of such magnetic NWs through their interactions with the host matrix is also of importance. In previous works, changes in the magnetic properties of Ni NW arrays embedded into polycarbonate (PC) membranes have been reported at low temperature as a result of the large thermal expansion coefficient mismatch between the polymer membrane and the Ni NWs.<sup>8–10)</sup> However, microwave devices operating in a temperature-controlled environment are far from adequate since they may require robust and energy-intensive cryogenic systems. Therefore, it is of paramount importance to enable external control of the matrix-dominated nanocomposite magnetic properties in order to design frequency agile microwave devices operating at room temperature.

In this work, we present a new route to control the magnetic properties of such arrays of ferromagnetic NWs by the electrochemical pore filling of ferroelectric poly(vinylidene difluoride) (PVDF) polymer templates rich in polar  $\beta$  form, resulting in the fabrication of multiferroic nanostructured composites. In such two-phase composite materials, a magnetoelectric effect may arise from a mechanical coupling between the magnetostrictive and piezoelectric phases. Indeed, the application of an electric field induces a stress on the piezoelectric constituent that is passed onto the magnetostrictive ferromagnet. It should be mentioned that evidence for multiferroic behavior was previously demonstrated in multilayered composite material made of PVDF and ferromagnetic layers.<sup>11)</sup> In order to enhance this coupling, the interfacial area between the two phases should be maximized. This can be accomplished by considering such rationally designed nanoscale composites based on NWs, which have a large surface to volume ratio. We report on an experimental study by ferromagnetic resonance (FMR) at room temperature for the magnetoelectric effect of Ni NWs

embedded in PVDF membranes. COMSOL Multiphysics was used to simulate the magnitude and spatial distribution of the electric field surrounding individual Ni NWs in the array. Shear piezoelectric effects are found from the simulations in the PVDF matrix surrounding the lateral surface of the NWs and are most probably associated with the weakening of the magnetic anisotropy along the NW easy axis, as observed experimentally.

We used a commercially available 28- $\mu\text{m}$ -thick PVDF film to produce track-etched ferroelectric polymer membranes using a process similar to that for the PC membrane.<sup>12)</sup> The PVDF film was uniaxially stretched and poled by the producer prior to the track-etching process. The pore size and pore density are 105 nm and  $2 \times 10^8 \text{ cm}^{-2}$ , respectively. For comparison, 22- $\mu\text{m}$ -thick PC templates with similar porosities were also made. Prior to electrodeposition, a metallic layer consisting of 20 nm Cr and 300 nm Au is deposited by evaporation on one face of the template, serving as the cathode. Details of the electrodeposition of Ni and permalloy ( $\text{Py} = \text{Ni}_{80}\text{Fe}_{20}$ ) NWs into the pores of polymer membranes can be found elsewhere.<sup>9)</sup> The experimental method for FMR measurements involves the measurement of the transmission coefficient of an incident microwave signal propagating along a microstrip line deposited on one face of a magnetically filled porous membrane (Fig. 1). More details of the arrangement can be found elsewhere.<sup>13)</sup> An adjustable bias voltage up to 200 V is applied through the two electrode pads on the microstrip line structure. Both positive and negative voltages were applied to the microstrip line while the cathode was maintained at zero potential.

The finite element method with COMSOL Multiphysics has been used to simulate the magnitude and spatial distribution of the static electric field from the bias voltage surrounding individual Ni NWs in the array. In Fig. 1, the calculated electric field lines are also shown. The electric field surrounding the end of each NW is strongly enhanced by the tip effect and radially distributed field lines appear in the neighborhood of the NW apex. Below the NW tip, the electric field is mostly aligned perpendicular to the NW axis. In Figs. 2(a) and 2(b), the calculated spatial variation of electric field intensity is shown by considering separately the vertical component (i.e., the axial direction of the NW) and

\*E-mail address: luc.piriaux@uclouvain.be

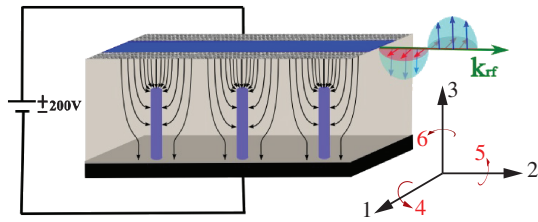


**Fig. 1.** Schematic description of the microstrip transmission line consisting of a metallic ground plane (and cathode), a ferroelectric PVDF polymer template filled with magnetic NWs and the 500 μm wide metallic microstrip line. An adjustable bias voltage up to ±200 V is applied through the two electrode pads. The calculated electric field lines due to this bias are indicated, as well as the definition of piezoelectric axes.

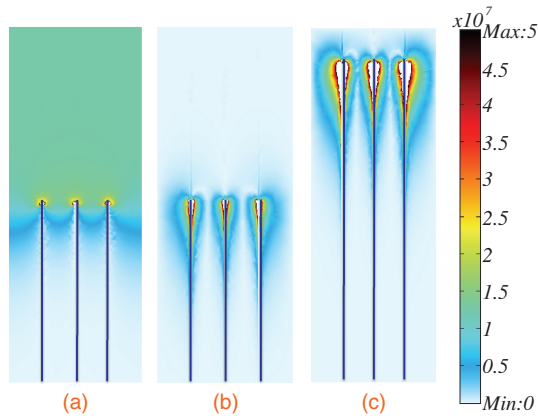


**Fig. 2.** Spatial distribution of electric field intensity in a PVDF–Ni NW nanocomposite ( $P = 0.16\%$ ,  $h_{Ni} = 0.5$ ) obtained by considering separately (a) the vertical component and (b) one component of the field in the plane of the PVDF film; (c) same as in (b) with  $h_{Ni} = 0.9$ . The color scale represents the magnitude of the field in V/m.

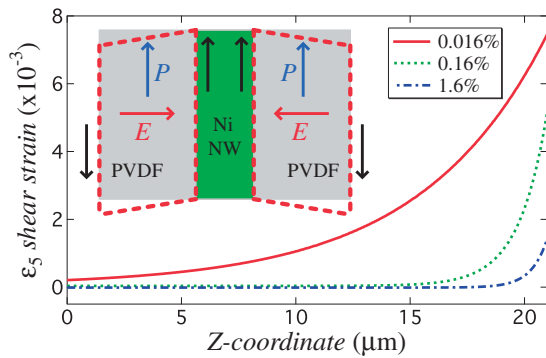
one component of the field in the plane of the PVDF film for a normalized filling height  $h_{Ni} = 0.5$  of the electrodeposited Ni NWs. The packing factor  $P$  of the array (defined as the cross-sectional area of the NWs) was fixed to 0.16% and the applied voltage was 200 V. The calculations reported in Fig. 2(a) show that the field penetration between parallel standing NWs is poor due to the proximity between neighboring NWs so the large height of the NWs compared with interwire distance leads to an electrostatic screening effect. As shown in Fig. 2(b), the electric field is mostly directed perpendicular to the NW axis in the region surrounding the lateral surface of the NWs. It is most intense at the tip and its magnitude decays rapidly underneath the NW extremity. As expected, the field intensity increases in the upper part of the NWs as the relative height of the NWs is larger, e.g.,  $h_{Ni} = 0.9$ , as shown in Fig. 2(c).

It is interesting to note that in the region surrounding the lateral surface of the NWs, the electric field has a large component perpendicular to the PVDF polar axis, denoted as “3”, which is perpendicular to the surface of the film, (Fig. 1). Therefore, shear occurs and the large shear piezoelectricity components  $d_{15}$  and  $d_{24}$  in PVDF are related to the strain induced by the perpendicular electric field as follows:  $\epsilon_5 = d_{15}E_1$  and  $\epsilon_4 = d_{24}E_2$ . In the above notations, the stretching direction of the film is denoted as “1”. The “2” axis is orthogonal to the stretching direction in the plane

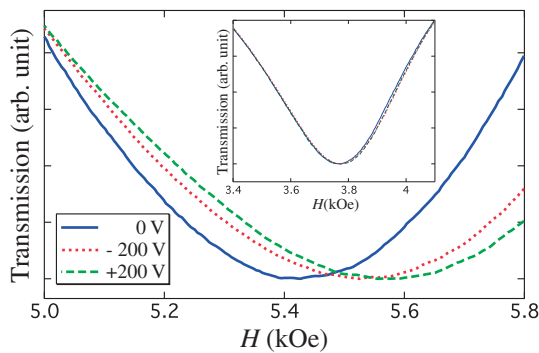
of the film. The shear planes, indicated by the subscripts “4” and “5”, are perpendicular to the directions “1” and “2”.<sup>14</sup> The inset of Fig. 3 shows a schematic representation of the shear strain in the PVDF matrix close to the nanowire tip, with displacements of the polymer surface along the polarization direction and no piezoelectric deformation along the electric field direction. From the quantitative determination of the electric field distribution surrounding the NWs, we may calculate the resulting shear strain  $\epsilon_5$ . We used  $d_{15} \approx -25$  pC/N as a typical value for a uniaxially stretched PVDF film.<sup>15</sup> In Fig. 3, the magnitude of the shear strain  $\epsilon_5$  in the PVDF matrix surrounding the lateral surface of the NWs is shown along the NW axis for three different NW packing  $P$  values namely 0.016% (continuous line), 0.16% (dotted line), and 1.6% (dash-dotted line). In all cases, the shear strain is at its maximum at the extremity of the NWs. Furthermore, the decay length of the shear strain along the axis of the NW depends strongly on the NW packing. It varies from  $\approx 2 \mu\text{m}$  for  $P = 1.6\%$  up to almost the entire length of the NWs for  $P = 0.016\%$ .

Figure 4 shows some representative FMR transmission spectra recorded at 25 GHz in an array of Ni NWs ( $\phi = 105$  nm) by applying the external magnetic field parallel to the NWs. Results are shown for applied voltages of ±200 V as well as without bias electric field. At zero bias voltage, a good agreement is found for the resonance field  $H_r$  by considering the simple formula  $H_r = f_r/\gamma - H_{ms}$ , where  $H_{ms} = 2\pi M_s(1 - 3P) \approx 2.9$  kOe is the magnetostatic field including both shape and dipolar interaction terms,<sup>16</sup>  $f_r$  is the resonance frequency and  $\gamma = 3.09$  GHz kOe<sup>-1</sup> and  $M_s = 485$  emu cm<sup>-3</sup> are the gyromagnetic ratio and the saturation magnetization for Ni, respectively. Very similar shifts in resonance field towards a higher magnetic field of about 160 Oe are observed for both positive and negative voltages. Such an increase in resonance field  $\Delta H_r$  corresponds to a decrease in the resonance frequency  $\Delta f_r = \gamma \Delta H_r \approx 500$  MHz, and is consistent with a reduction in uniaxial magnetic anisotropy. This decrease is observed experimentally in the effective permeability of the nanowired substrate extracted from transmission and reflection measurements<sup>17</sup> in frequency-sweeping mode, for various values of DC biasing magnetic field: a shift of its FMR frequency towards lower frequencies occurs when a bias voltage is applied. FMR voltage tuning of permeability is present even in absence of DC magnetic field. This is of prime interest for reconfigurable devices involved in wireless transceivers and antennas arrays: voltage-controlled oscillators (VCOs), circulators, differential phase shifters, etc., could be tuned between 5 GHz and 30 GHz depending on the nature of the ferromagnetic nanowires fixing FMR and on values of DC biasing voltage. Several NW-based nanocomposites have been investigated using FMR measurements. As expected, no shift in resonance field has been observed in a PVDF–Py sample (see the inset in Fig. 4), which is ascribed to the fact that permalloy has negligible magnetostriction.<sup>9,18</sup> It should be also emphasized that no E-field induced effects were found in PC–Ni samples in which the polymer matrix shows no piezoelectricity.

Even if the exact nature of the stress that is imposed on the NWs remains to be determined, it can be replaced by an equivalent field,  $H_{me}$ , the magneto-elastic component on the effective field, and will be of the order of<sup>19,20</sup>



**Fig. 3.** Variation of the calculated shear strain  $\epsilon_5$  in PVDF matrix surrounding the lateral surface of the NWs for three NW packing densities,  $P = 0.016, 0.16,$  and  $1.6\%$ , respectively. In all cases, the relative height of the Ni NWs,  $h_{\text{Ni}} = 0.75$ . The inset shows a schematic representation of the shear strain appearing in the PVDF matrix at the interface with a Ni nanowire with the black arrows indicating the strain orientation.



**Fig. 4.** Field sweep microwave absorption spectra recorded at 25 GHz with the field applied parallel to the NWs for an array of Ni NWs ( $\phi \approx 105$  nm,  $h_{\text{Ni}} \approx 0.75$ , and  $P = 1.6\%$ ) embedded in a PVDF membrane. Experimental data are shown for zero bias voltage applied (continuous line) as well as for non-zero values ( $V = +200$  V, dashed line;  $V = -200$  V, dotted line). The inset shows similar FMR transmission spectra for a PVDF-Py sample with  $\phi = 105$  nm and  $P = 1.6\%$ .

$$H_{\text{me}} = \frac{3\lambda E\epsilon}{2M_s}, \quad (1)$$

where  $\lambda$  is the magnetostriction coefficient ( $\lambda \approx -30 \times 10^{-6}$  for polycrystalline Ni NWs),  $E$  is the Young modulus of Ni (200 GPa) and  $\epsilon$  denotes the strain. The experimental values for the shift in resonance field measured in several PVDF-Ni samples are in the range 40–160 Oe. Using eq. (1), the changes in effective field correspond to strains in the range  $(2-8) \times 10^{-4}$ , which is consistent with the calculated values shown in Fig. 3 for the case  $P = 1.6\%$ . From the simulations shown in Fig. 3, it appears that for more diluted NW arrays, e.g.,  $P = 0.016\%$ , not only the strain is much larger at the tip (by a factor of 5), but also it expands over the whole length of the NW, so that one can anticipate that strongly enhanced shifts in resonance frequency, up to several GHz for the same applied voltage, should be observed. However, such low NW concentrations fall below the sensitivity threshold of conventional transmission line based FMR measurements.

Furthermore, it should be emphasized that the measured effects slightly depend on the polarity of the bias voltage, although the magnitude of the shift in resonance field towards a higher magnetic field for a selected sample may differ up to 25% at  $V = +200$  and  $-200$  V. A detailed analysis of the FMR results would require a refined theoretical model for the mechanical stress introduced by the piezoelectricity of PVDF and the resulting strain in the Ni NWs. This is however outside the scope of the present study.

To summarize, we have elaborated new multiferroic nanocomposites consisting of arrays of ferromagnetic Ni NWs embedded in ferroelectric PVDF nanoporous templates. From FMR shifts induced by static bias voltage, we demonstrate a magnetoelectric effect arising from a mechanical coupling between the high aspect ratio Ni NWs and the piezoelectric matrix. The calculated electric field lines and intensity indicate that the PVDF matrix surrounding the lateral surface of the Ni NWs experiences shear stress. The competing magnetoelastic anisotropy originating from the piezoelectric effects leads to a reduced magnetic anisotropy field along the NWs axis. Furthermore, it is found that the electric field-induced ferromagnetic resonance shifts are almost independent of the voltage polarity while no effects are observed in PVDF-Py and PC-Ni systems. Both interwire distance and relative height are crucial parameters in determining the magnitude of the magnetoelectric effect. We believe that this novel approach promises to be of strong interest as magnetic NW arrays embedded in dielectric substrates with tunable ferromagnetic resonance frequencies are highly desirable for agile microwave devices.

**Acknowledgments** This work was partly supported by the Interuniversity Attraction Poles Programs (P6/27 and P6/42)—Belgian State-Belgian Science Policy. I.H. is the Research Director of Research Science Foundation (FRS-FNRS), Belgium. G.H. is a Research Fellow of the National Fund for Training in Research in Industry and Agriculture (FRIA), Belgium. The authors would like to thank P. Simon for his help and advice, L. Jonckheere and M. Planckaert for the preparation of track-etched membranes and T. Pardoen for useful discussions. J. De La Torre thanks PROMEP for financial support through grant No. PROMEP/103.5/11/2159.

- 1) C. A. Ross: *Annu. Rev. Mater. Sci.* **31** (2001) 203.
- 2) J. F. Allaey and J. C. Mage: *J. Phys. D* **40** (2007) 3714.
- 3) B. K. Kuanr *et al.*: *Appl. Phys. Lett.* **94** (2009) 202505.
- 4) M. Darques *et al.*: *Nanotechnology* **21** (2010) 145208.
- 5) C. E. Carreon-Gonzalez *et al.*: *Nano Lett.* **11** (2011) 2023.
- 6) L. Piraux *et al.*: *Nano Lett.* **7** (2007) 2563.
- 7) N. Biziere *et al.*: *Phys. Rev. B* **79** (2009) 012404.
- 8) S. Dubois *et al.*: *Phys. Rev. B* **61** (2000) 14315.
- 9) J. De La Torre Medina *et al.*: *J. Phys. D* **41** (2008) 032008.
- 10) A. Ghaddar *et al.*: *Acta Phys. Pol.* **116** (2009) 1039.
- 11) F. Rasoanoavy *et al.*: *J. Appl. Phys.* **107** (2010) 09E313.
- 12) E. Ferain and R. Legras: *Nucl. Instrum. Methods Phys. Res., Sect. B* **208** (2003) 115.
- 13) G. Goglio *et al.*: *Appl. Phys. Lett.* **75** (1999) 1769.
- 14) R. G. Kepler: in *Ferroelectric Polymers: Chemistry, Physics, and Applications*, ed. H. Singh Nalwa (Marcel Dekker, New York, 1995).
- 15) E. L. Nix and I. M. Ward: *Ferroelectrics* **67** (1986) 137.
- 16) A. Encinas Oropesa *et al.*: *Phys. Rev. B* **63** (2001) 104415.
- 17) J. Spiegel and I. Huynen: *J. Comput. Theor. Nanosci.* **6** (2009) 2001.
- 18) R. Bonin *et al.*: *J. Appl. Phys.* **98** (2005) 123904.
- 19) A. Kumar *et al.*: *Phys. Rev. B* **73** (2006) 064421.
- 20) B. D. Cullity and C. D. Graham, Jr.: *Introduction to Magnetic Materials* (Wiley-IEEE Press, Piscataway, NJ, 2009).